Engineering Proximity Exchange by Twisting: Reversal of Ferromagnetic and Emergence of Antiferromagnetic Dirac Bands in Graphene/$Cr_2Ge_2Te_6$

Klaus Zollner[*] and Jaroslav Fabian

Institute for Theoretical Physics, University of Regensburg, 93040 Regensburg, Germany

We investigate the twist-angle and gate dependence of the proximity exchange coupling in twisted graphene on monolayer $Cr_2Ge_2Te_6$ from first principles. The proximitized Dirac band dispersions of graphene are fitted to a model Hamiltonian, yielding effective sublattice-resolved proximity-induced exchange parameters (λ_{ex}^A and λ_{ex}^B) for a series of twist angles between 0° and 30°. For aligned layers (0° twist angle), the exchange coupling of graphene is the same on both sublattices, $\lambda_{ex}^A \approx \lambda_{ex}^B \approx 4$ meV, while the coupling is reversed at 30° (with $\lambda_{ex}^A \approx \lambda_{ex}^B \approx -4$ meV). Remarkably, at 19.1° the induced exchange coupling becomes antiferromagnetic: $\lambda_{ex}^A < 0$, $\lambda_{ex}^B > 0$. Further tuning is provided by a transverse electric field and the interlayer distance. The predicted proximity magnetization reversal and emergence of an antiferromagnetic Dirac dispersion make twisted graphene/$Cr_2Ge_2Te_6$ bilayers a versatile platform for realizing topological phases and for spintronics applications.

Van der Waals (vdW) heterostructures composed of twisted monolayers [1–4] promise great tunability of electronic, optical, and magnetic properties. The most prominent example is magic-angle twisted bilayer graphene, exhibiting magnetism and superconductivity due to strong correlations [5–19]. Other platforms for correlated physics are offered by trilayer graphene [20–29] and twisted transition metal dichalcogenides (TMDCs) [30].

However, twistronics has yet to demonstrate its potential for proximity effects [31], enabling phenomena such as superconductivity [32,33], magnetism [34–52], and strong spin-orbit coupling (SOC) [53–69] in materials—most notably graphene—lacking them. Magnetism in graphene can be induced by proximity exchange coupling with a ferro- or antiferromagnet. Of particular interest are magnetic insulators (semiconductors) such as $Cr_2Ge_2Te_6$ [39,58,70] (CGT) or CrI_3 [40,49,71,72], which can modulate the band structure of graphene (or another nonmagnetic material) without significant charge transfer and without contributing additional transport channels. Proximity exchange effects in graphene can be observed by quantum anomalous Hall effect [73], magnetoresistance [74], or nonlocal spin transport experiments [75]. Joined with strong SOC in ex-so-tic heterostructures [76,77] proximity exchange can also induce spin-orbit torque [70,78–80].

We already know that proximity exchange coupling in graphene can be tuned by gate [34,81]. Can we also tune it by twisting? A recent study shows the sensitivity of the spin polarization, magnetic anisotropy, and Dzyaloshinskii-Moriya interaction to the twist angle in graphene/2H-VSeTe heterostructures [82]. Similarly, tight-binding studies predict that the strength of proximity SOC in graphene/TMDC heterostructures [83,84] can be tuned by the twist angle. It is then natural to expect that the strength of the proximity exchange could change depending on the twist angle.

We show here that not only the magnitude, but also the orientation and even the character (ferro- or antiferromagnetic) of the proximity exchange can depend on the twist angle. Employing first-principles calculations, we study the twist-angle dependence of the proximity exchange coupling in large graphene/CGT supercells. From the proximitized Dirac band dispersions of graphene, which we fit to a model Hamiltonian, we extract sublattice-resolved exchange parameters λ_{ex}^A and λ_{ex}^B for a series of twist angles between 0° and 30°. We find that one can tune the ferromagnetic (uniform) exchange couplings ($\lambda_{ex}^A \approx \lambda_{ex}^B$) from about 4 to −4 meV by twisting the layers. This reversal of the induced spin polarization by the twist angle is surprising when considering that the CGT magnetization orientation is unchanged.

Even more surprising is the emergence of antiferromagnetic (staggered) proximity exchange coupling at 19.1°, where $\lambda_{ex}^A < 0$ and $\lambda_{ex}^B > 0$. At this twist angle there is a delicate balance in the orbital hybridization of the spin-up and spin-down CGT bands with the carbon p_z orbitals, which makes the exchange coupling highly sensitive to the atomic registry. By laterally shifting the two layers, ferromagnetic couplings can be realized as well. Graphene/CGT stacks thus form a versatile platform for engineering proximity exchange coupling in graphene.

Finally, we also study the influence of strain, interlayer distance, and (transverse) electric field on the doping level, band offsets, and proximity exchange parameters, for different twist angles. We point out the crucial role of

both momentum backfolding and interlayer orbital hybridization when tracing the microscopic mechanism for the observed proximity exchange tunability. One important message that our results convey is that the knowledge of the twist angle is crucial when reporting experiments on magnetic proximity effects: not only the orientation of the induced spin polarization, but also the apparent magnetic ordering (ferro- or antiferromagnetic) need not correspond to the substrate magnetic layer.

Crystal structures.—We consider vdW heterostructures of graphene and CGT, with a series of twist angles, ranging from 0° to 30° in steps of roughly 3°, between the two monolayers, see Fig. 1. In order to form commensurate supercells for periodic density-functional theory (DFT) calculations, we strain the monolayers in the twisted heterostructures. In Table S1 we summarize the main structural information for the twist angles we consider, see Supplemental Material [85]. After relaxation of the heterostructures, we find an average interlayer distance $d_{int} \approx 3.55$ Å and a graphene rippling $\Delta z_{grp} < 1$ pm nearly independent of the twist angle.

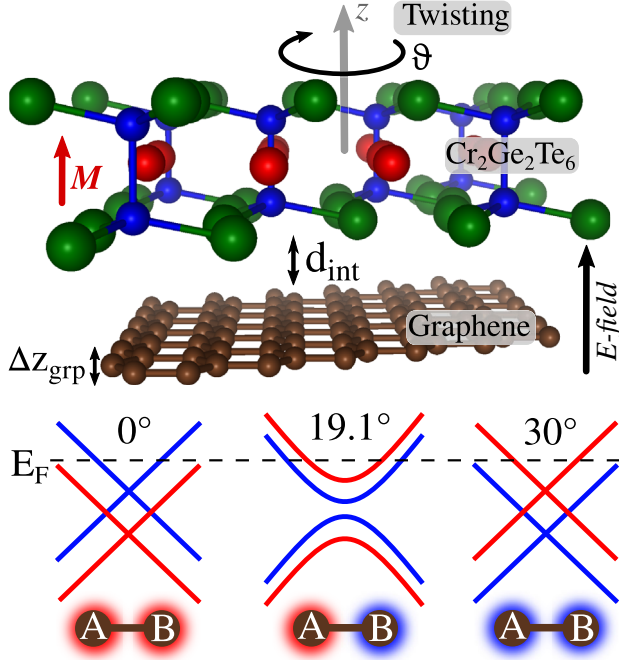*Effective low-energy Hamiltonian.*—From our first-principles calculations we extract the low-energy band

FIG. 1. 3D view of CGT on graphene, where we define the interlayer distance d_{int} and the rippling of the graphene layer Δz_{grp}. We twist CGT by an angle ϑ around the z axis, with respect to graphene. The proximitized Dirac dispersions are sketched for three most relevant twist angles. Red bands are polarized spin-up (defined by the CGT magnetization M along z direction), while blue bands are polarized spin-down. The spin polarizations on the graphene lattice, resulting from these Dirac bands at the given Fermi level (dashed line), are also sketched.

structure of the proximitized graphene. The systems we consider have broken time-reversal symmetry with C_3 structural symmetry. The following Hamiltonian, derived from symmetry [34,110,111], is able to describe the graphene bands in the vicinity of the Dirac points when proximity exchange is present:

$$\mathcal{H} = \mathcal{H}_0 + \mathcal{H}_\Delta + \mathcal{H}_{ex} + E_D, \quad (1)$$

$$\mathcal{H}_0 = \hbar v_F (\tau k_x \sigma_x - k_y \sigma_y) \otimes s_0, \quad (2)$$

$$\mathcal{H}_\Delta = \Delta \sigma_z \otimes s_0, \quad (3)$$

$$\mathcal{H}_{ex} = (-\lambda_{ex}^A \sigma_+ + \lambda_{ex}^B \sigma_-) \otimes s_z. \quad (4)$$

Here v_F is the Fermi velocity and the in-plane wave vector components k_x and k_y are measured from $\pm K$, corresponding to the valley index $\tau = \pm 1$. The Pauli spin matrices are s_i, acting on spin space $(\uparrow, \downarrow)$, and σ_i are pseudospin matrices, acting on sublattice space (C_A, C_B), with $i = \{0, x, y, z\}$ and $\sigma_\pm = \frac{1}{2}(\sigma_z \pm \sigma_0)$. The staggered potential gap is Δ and the sublattice-resolved proximity-induced exchange parameters are λ_{ex}^A and λ_{ex}^B. The four basis states are $|\Psi_A, \uparrow\rangle$, $|\Psi_A, \downarrow\rangle$, $|\Psi_B, \uparrow\rangle$, and $|\Psi_B, \downarrow\rangle$. The model Hamiltonian is valid close to the Fermi level at zero energy. Charge transfer between the monolayers in the DFT calculation is captured by the Dirac point energy E_D, which adjusts the Dirac point with respect to the Fermi level.

Proximity-induced exchange in twisted structures.—In Fig. 2(a), we show the global band structure for the graphene/CGT heterostructure for a twist angle of 30°; the results for other angles and effects of interlayer charge transfer are summarized in the Supplemental Material [85]. In agreement with recent calculations [39,58,70], we find the Dirac cone located at the Fermi level and close to the conduction-band edge of the CGT.

In Figs. 2(b)–2(d) we present enlargements to the Dirac bands, which exhibit proximity exchange splitting, along with the calculated spin polarizations on graphene. For the aligned heterostructure (0°) the exchange splitting is ferromagnetic, with uniform spin polarization on A and B sublattices. The fitted exchange parameters are $\lambda_{ex}^A \approx \lambda_{ex}^B \approx 4.2$ meV. The Dirac bands look similar for the 30° twist angle, but the spin polarization on graphene is *reversed*, with the parameter values of $\lambda_{ex}^A \approx \lambda_{ex}^B \approx -3.6$ meV. This is rather surprising considering that the ferromagnet in both cases has the same magnetization orientation.

However, the most remarkable case is the 19.1° twist angle, shown in Fig. 2(c). The Dirac band structure does not resemble a ferromagnetic graphene at all. Instead, the spin splittings of the bands are compatible with *antiferromagnetic* exchange. Indeed, a fit to the low-energy Hamiltonian (1) yields staggered exchange couplings, $\lambda_{ex}^A \approx -2.1$ and
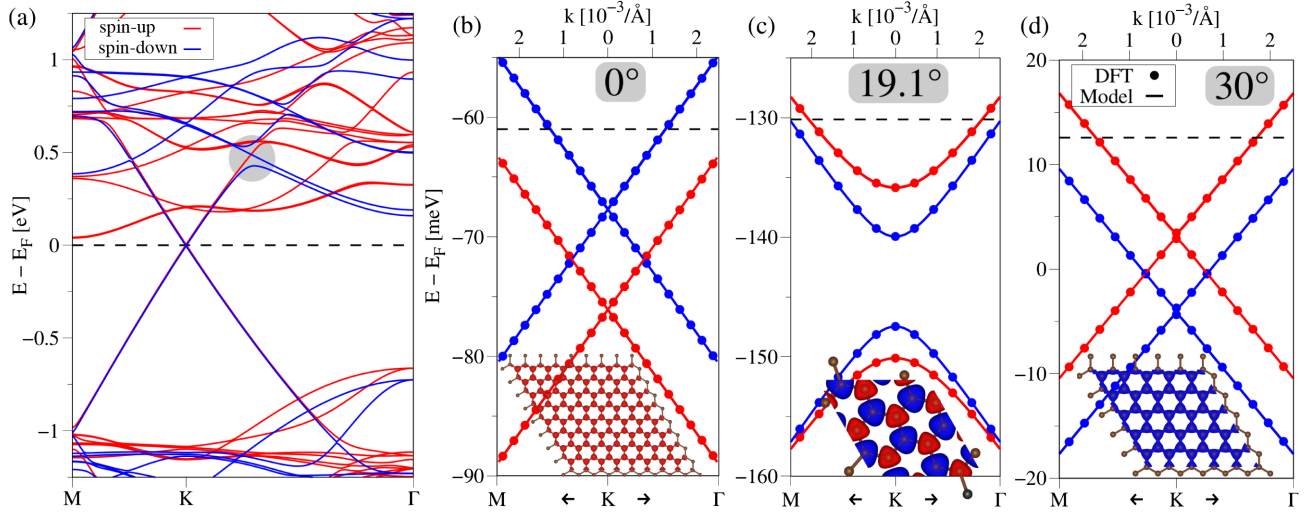
FIG. 2. (a) DFT-calculated band structure of the graphene/CGT heterostructure along the high-symmetry path M-K-Γ for a twist angle of 30°. Red (blue) solid lines correspond to spin-up (spin-down). Gray disk indicates anticrossing of Dirac and CGT bands. (b) Enlargement of the DFT-calculated (symbols) low-energy Dirac bands near the K point with a fit to the model Hamiltonian (solid lines) for a twist angle of 0°. Inset: the calculated spin polarization on graphene, considering Dirac states in the energy window of about ± 2.5 meV around the indicated Fermi level (dashed line). (c),(d) Same as (b), but for 19.1° and 30°.

$\lambda_{\mathrm{ex}}^{B} \approx 1.3$ meV. In other words, graphene proximitized by a ferromagnetic substrate can behave as an antiferromagnet, with alternating spin polarization on A and B sublattices.

To get the full picture of proximity exchange, we plot in Fig. 3 the twist-angle dependence of ferromagnetic $\lambda_{\mathrm{F}} = (\lambda_{\mathrm{ex}}^{A} + \lambda_{\mathrm{ex}}^{B})/2$ and antiferromagnetic $\lambda_{\mathrm{AF}} = (\lambda_{\mathrm{ex}}^{A} - \lambda_{\mathrm{ex}}^{B})/2$ couplings (listed in Tables S2 and S4 [85]); the magnetization of CGT is kept in the same direction for all studied angles. We find a rather continuous tunability of the ferromagnetic exchange from 4 to −4 meV, when twisting from 0° to 30°. Antiferromagnetic exchange emerges only at 19.1°. Figure 3 also shows data for structures, where only graphene is strained (CGT is kept unstrained), to
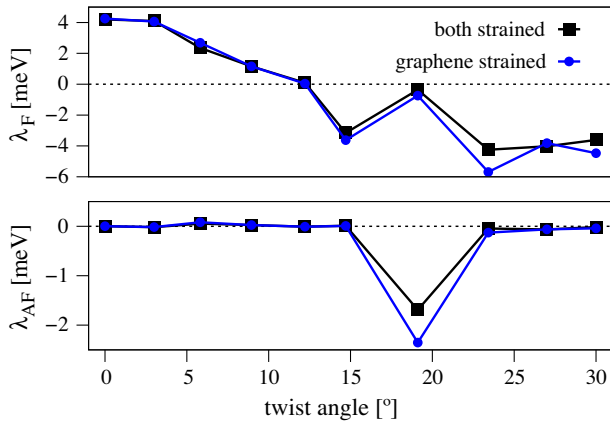
demonstrate the robustness of these findings against strain; we note that strain controls mainly the band offsets and related charge transfer, see Supplemental Material [85].

Tunability by electric field.—We now consider the graphene/CGT stacks with different twist angles and apply a transverse electric field between ± 1.5 V/nm. The positive direction of the field is indicated in Fig. 1. We wish to answer the question: Can one tune the proximity-induced exchange coupling by gating?
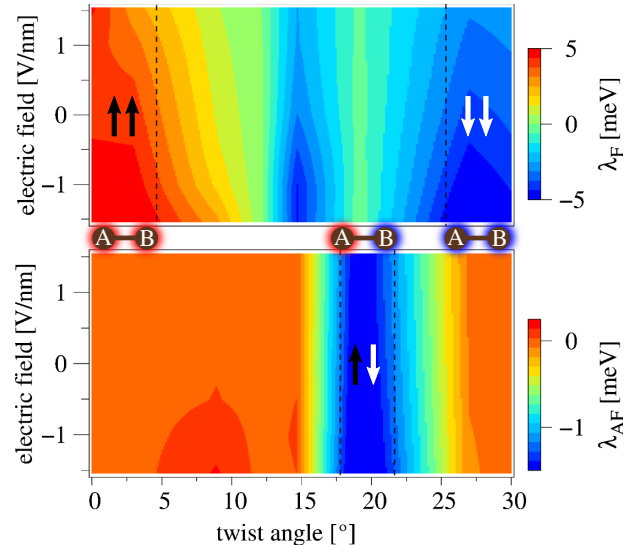

FIG. 3. Calculated twist-angle dependence of the (top) ferromagnetic λ_{F} and (bottom) antiferromagnetic λ_{AF} proximity exchange coupling of the graphene/CGT bilayers. We summarize the results for heterostructures with both layers strained and with only graphene strained.

FIG. 4. Calculated electric-field and twist-angle dependence of the (top) ferromagnetic λ_{F} and (bottom) antiferromagnetic λ_{AF} proximity-induced exchange coupling (interpolated from Table S5 [85]). Vertical dashed lines indicate regions of strong ferro- or antiferromagnetic exchange. The spin polarizations on the graphene lattice are sketched (see also Fig. 1).

In Fig. 4 we summarize the calculated electric-field and twist-angle dependence of the proximity-induced ferromagnetic and antiferromagnetic exchange coupling, as listed in Table S5 [85]. While the qualitative picture of spin-polarization reversal at 30° and appearance of anti-ferromagnetic polarization at 19.1° remains unchanged, the applied electric field can tune the proximity magnetization rather significantly for some twist angles. A striking example is the 12.2° twist angle: Even though the proximity exchange parameters are small, they can be tuned from positive to negative by the gate field. The antiferromagnetic proximity exchange at 19.1° stays, but is weakly tunable by the field. Overall, we find that both gating and twisting are two efficient knobs to tailor the signs and magnitudes of the proximity-induced exchange couplings in graphene/CGT bilayers. We expect similar tunabilities (although at different twist angles) for other graphene/ferromagnetic-insulator heterostructures.

Sensitivity to interlayer distance and atomic registry.— We find that the interlayer distance strongly influences the proximity exchange, see Table S6 [85]. Tuning d_{int} by ± 0.1 Å, the exchange parameters can be tuned by about $\mp 30\%$. Such tunability has recently been measured for the proximity SOC in graphene/WSe$_2$ heterostructures [69,86]. The atomic registry does not play a role for proximity exchange couplings for 0° and 30° twist angles. However, as we show in the Supplemental Material [85], shifting the layers relative to each other, while keeping the twist angle at 19.1°, one can get both staggered and uniform exchange couplings. At this angle the heterostructure supercell is relatively small (24 atoms), making the proximity exchange coupling particularly sensitive to the atomic registry. Further encapsulation of graphene within two CGT layers provides additional boost and tailoring of proximity exchange, see [85].

Mechanism of twist-angle dependence of proximity exchange.—The twist-angle dependence of proximity SOC in graphene/TMDC heterostructures has been explained by downfolding the tight-binding model of coupled bilayers [83,84]. The main mechanism there is the tunability of the interlayer interaction connecting the graphene K point with TMDC Bloch states at different k points for different twist angles. Comparison with recent large scale DFT calculations [112,113] points to the importance of both spectral variations of the TMDC band structure in the Brillouin zone, but also of the interlayer orbital hybridization.

Can we deduce the rather striking reversal of the spin polarization of the Dirac electrons by considering the spectral variations only? The calculated spin-resolved electronic band structure of monolayer CGT, with back-folded graphene K points, is shown in Fig. 5. Second-order perturbation theory predicts level repulsion, so considering energy bands only, Fig. 5 indicates for 0° that spin-up Dirac bands are pushed above spin-down bands, and vice versa
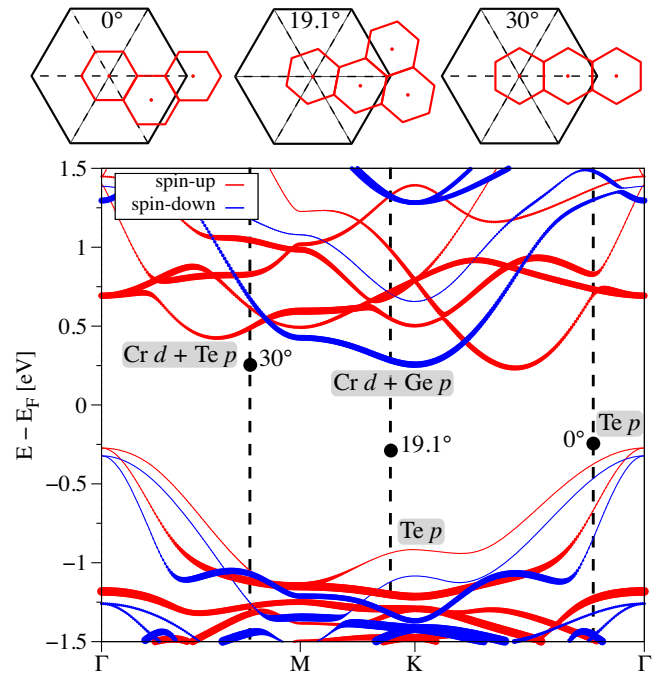

FIG. 5. Top: Backfolding of the graphene Dirac point at K to k points of CGT for different twist angles. The black (red) hexagons represent the graphene (CGT) Brillouin zones. Bottom: The DFT-calculated band structure of monolayer CGT, where the vertical dashed lines indicate the k points, to which the Dirac states couple to, according to the backfolding. The black dots are the locations of the Dirac point for the different twist angles from Table S4 [85], when CGT is unstrained. We also indicate the main orbital contribution of the bands close to the black dots. The line thicknesses are weighted by the sum of projections onto z-extended orbitals (Te p_z, Ge p_z, and Cr $d_{z^2} + d_{xz+yz}$).

for 30°. This is opposite to what is predicted in Figs. 2(b) and 2(d).

The CGT bands in Fig. 5 are weighted by their z-like orbitals content. Those are most likely to overlap with the lobes of graphene's p_z orbitals. There does not appear any discernable pattern here that would predict the DFT-calculated behavior in Fig. 2. But what Fig. 5 does reveal is that one would need to consider many bands—and both the energies and overlaps with Dirac band p_z orbitals— around the CGT gap at the corresponding backfolded K point, to be able to reproduce the DFT results. For example, for 0° the nearest valence bands are formed by Te $p_x + p_y$ orbitals whose overlap with graphene p_z is weak. We elaborate more on this point in the Supplemental Material (see Fig. S19) [85].

The relevance of high-energy bands for the spin polarization at the Dirac point is revealed by the heterostructure dispersion of, for example, the 30° structure in Fig. 2(a). One finds a pronounced anticrossing (gray disk) signaling a particularly strong coupling of spin-down carbon p_z orbitals and the lowest CGT spin-down conduction-band states (formed by Ge p_z and Cr d orbitals). This coupling,

which is nicely seen in the density plots in Fig. S12 [85], justifying the effective model Hamiltonian, lowers the spin-down more than spin-up Dirac states, in agreement with Fig. 2(d). Even though the anticrossing is at about 500 meV above the Dirac point, the corresponding high-lying CGT band provides a sizable spin splitting of the Dirac band structure due to the strong coupling. Similar observations hold for 0° and 19.1° cases, see Supplemental Material [85].

Since the heterostructure unit cells comprise many carbon atoms, it is not obvious that the calculated spin-split Dirac bands, which arise due to couplings to high-lying CGT bands, map to a local proximity magnetization pattern in the graphene layer. The DFT-calculated local spin polarizations of the conduction-band electrons in proximitized graphene are plotted as insets in Figs. 2(b)–2(d). There is a perfect correspondence between the spin-split bands and the local spin-polarization pattern—with the emerging pseudospin-resolved polarization—justifying our effective Hamiltonian (1).

Conclusions.—Employing DFT on large supercells, we show that one can engineer the proximity exchange of Dirac electrons in graphene/CGT stacks by twisting, which should be useful for spin transport experiments—spin Hanle effect, spin relaxation anisotropy, spin torque—as well as for realizing topological states [40,87,114] requiring both SOC and (ferro- or antiferromagnetic) exchange in graphene. Our results also stress the importance of documenting the twist angle when employing magnetic vdW heterostructures in experiments.

---

[*]klaus.zollner@physik.uni-regensburg.de

[1] Stephen Carr, Daniel Massatt, Shiang Fang, Paul Cazeaux, Mitchell Luskin, and Efthimios Kaxiras, Twistronics: Manipulating the electronic properties of two-dimensional layered structures through their twist angle, Phys. Rev. B **95**, 075420 (2017).

[2] Zachariah Hennighausen and Swastik Kar, Twistronics: A turning point in 2d quantum materials, Electronic structure and magnetism of inorganic compounds **3**, 014004 (2021).

[3] Rebeca Ribeiro-Palau, Changjian Zhang, Kenji Watanabe, Takashi Taniguchi, James Hone, and Cory R. Dean, Twistable electronics with dynamically rotatable heterostructures, Science **361**, 690 (2018).

[4] Stephen Carr, Shiang Fang, and Efthimios Kaxiras, Electronic-structure methods for twisted moiré layers, Nat. Rev. Mater. **5**, 748 (2020).

[5] Yuan Cao, Valla Fatemi, Shiang Fang, Kenji Watanabe, Takashi Taniguchi, Efthimios Kaxiras, and Pablo Jarillo-Herrero, Unconventional superconductivity in magic-angle graphene superlattices, Nature (London) **556**, 43 (2018).

[6] Yuan Cao, Valla Fatemi, Ahmet Demir, Shiang Fang, Spencer L. Tomarken, Jason Y. Luo, Javier D. Sanchez-Yamagishi, Kenji Watanabe, Takashi Taniguchi, Efthimios Kaxiras, Ray C. Ashoori, and Pablo Jarillo-Herrero, Correlated insulator behaviour at half-filling in magic-angle graphene superlattices, Nature (London) **556**, 80 (2018).

[7] Harpreet Singh Arora, Robert Polski, Yiran Zhang, Alex Thomson, Youngjoon Choi, Hyunjin Kim, Zhong Lin, Ilham Zaky Wilson, Xiaodong Xu, Jiun-Haw Chu *et al.*, Superconductivity in metallic twisted bilayer graphene stabilized by WSe$_2$, Nature (London) **583**, 379 (2020).

[8] Petr Stepanov, Ipsita Das, Xiaobo Lu, Ali Fahimniya, Kenji Watanabe, Takashi Taniguchi, Frank HL Koppens, Johannes Lischner, Leonid Levitov, and Dmitri K. Efetov, Untying the insulating and superconducting orders in magic-angle graphene, Nature (London) **583**, 375 (2020).

[9] Xiaobo Lu, Petr Stepanov, Wei Yang, Ming Xie, Mohammed Ali Aamir, Ipsita Das, Carles Urgell, Kenji Watanabe, Takashi Taniguchi, Guangyu Zhang *et al.*, Superconductors, orbital magnets and correlated states in magic-angle bilayer graphene, Nature (London) **574**, 653 (2019).

[10] Aaron L. Sharpe, Eli J. Fox, Arthur W. Barnard, Joe Finney, Kenji Watanabe, Takashi Taniguchi, M. A. Kastner, and David Goldhaber-Gordon, Emergent ferromagnetism near three-quarters filling in twisted bilayer graphene, Science **365**, 605 (2019).

[11] Yu Saito, Fangyuan Yang, Jingyuan Ge, Xiaoxue Liu, Takashi Taniguchi, Kenji Watanabe, JIA Li, Erez Berg, and Andrea F. Young, Isospin Pomeranchuk effect in twisted bilayer graphene, Nature (London) **592**, 220 (2021).

[12] M. Serlin, C. L. Tschirhart, H. Polshyn, Y. Zhang, J. Zhu, K. Watanabe, T. Taniguchi, L. Balents, and A. F. Young, Intrinsic quantized anomalous Hall effect in a moiré heterostructure, Science **367**, 900 (2020).

[13] Amol Nimbalkar and Hyunmin Kim, Opportunities and challenges in twisted bilayer graphene: A review, Nano-Micro Lett. **12**, 126 (2020).

[14] Nick Bultinck, Shubhayu Chatterjee, and Michael P. Zaletel, Mechanism for Anomalous Hall Ferromagnetism in Twisted Bilayer Graphene, Phys. Rev. Lett. **124**, 166601 (2020).

[15] Cécile Repellin, Zhihuan Dong, Ya-Hui Zhang, and T. Senthil, Ferromagnetism in Narrow Bands of Moiré Superlattices, Phys. Rev. Lett. **124**, 187601 (2020).

[16] Youngjoon Choi, Jeannette Kemmer, Yang Peng, Alex Thomson, Harpreet Arora, Robert Polski, Yiran Zhang, Hechen Ren, Jason Alicea, Gil Refael *et al.*, Electronic correlations in twisted bilayer graphene near the magic angle, Nat. Phys. **15**, 1174 (2019).

[17] Simone Lisi, Xiaobo Lu, Tjerk Benschop, Tobias A. de Jong, Petr Stepanov, Jose R. Duran, Florian Margot, Irène Cucchi, Edoardo Cappelli, Andrew Hunter *et al.*, Observation of flat bands in twisted bilayer graphene, Nat. Phys. **17**, 189 (2021).

[18] Leon Balents, Cory R. Dean, Dmitri K. Efetov, and Andrea F. Young, Superconductivity and strong correlations in moiré flat bands, Nat. Phys. **16**, 725 (2020).

[19] T. M. R. Wolf, J. L. Lado, G. Blatter, and O. Zilberberg, Electrically Tunable Flat Bands and Magnetism in Twisted Bilayer Graphene, Phys. Rev. Lett. **123**, 096802 (2019).

[20] Ziyan Zhu, Stephen Carr, Daniel Massatt, Mitchell Luskin, and Efthimios Kaxiras, Twisted Trilayer Graphene: A Precisely Tunable Platform for Correlated Electrons, Phys. Rev. Lett. **125**, 116404 (2020).

[21] Jeong Min Park, Yuan Cao, Kenji Watanabe, Takashi Taniguchi, and Pablo Jarillo-Herrero, Tunable strongly coupled superconductivity in magic-angle twisted trilayer graphene, Nature (London) **590**, 249 (2021).

[22] Guorui Chen, Lili Jiang, Shuang Wu, Bosai Lyu, Hongyuan Li, Bheema Lingam Chittari, Kenji Watanabe, Takashi Taniguchi, Zhiwen Shi, Jeil Jung *et al.*, Evidence of a gate-tunable Mott insulator in a trilayer graphene moiré superlattice, Nat. Phys. **15**, 237 (2019).

[23] Guorui Chen, Aaron L. Sharpe, Eli J. Fox, Ya-Hui Zhang, Shaoxin Wang, Lili Jiang, Bosai Lyu, Hongyuan Li, Kenji Watanabe, Takashi Taniguchi *et al.*, Tunable correlated Chern insulator and ferromagnetism in a moiré super-lattice, Nature (London) **579**, 56 (2020).

[24] Guorui Chen, Aaron L. Sharpe, Patrick Gallagher, Ilan T. Rosen, Eli J. Fox, Lili Jiang, Bosai Lyu, Hongyuan Li, Kenji Watanabe, Takashi Taniguchi *et al.*, Signatures of tunable superconductivity in a trilayer graphene moiré superlattice, Nature (London) **572**, 215 (2019).

[25] Haoxin Zhou, Tian Xie, Areg Ghazaryan, Tobias Holder, James R. Ehrets, Eric M. Spanton, Takashi Taniguchi, Kenji Watanabe, Erez Berg, Maksym Serbyn *et al.*, Half- and quarter-metals in rhombohedral trilayer graphene, Nature (London) **598**, 429433 (2021).

[26] Yang-Zhi Chou, Fengcheng Wu, Jay D. Sau, and Sankar Das Sarma, Acoustic-Phonon-Mediated Superconductivity in Rhombohedral Trilayer Graphene, Phys. Rev. Lett. **127**, 187001 (2021).

[27] Võ Tien Phong, Pierre A. Pantaleón, Tommaso Cea, and Francisco Guinea, Band structure and superconductivity in twisted trilayer graphene, Phys. Rev. B **104**, L121116 (2021).

[28] Haoxin Zhou, Tian Xie, Takashi Taniguchi, Kenji Watanabe, and Andrea F. Young, Superconductivity in rhombohedral trilayer graphene, Nature (London) **598**, 434438 (2021).

[29] Wei Qin and Allan H. MacDonald, In-Plane Critical Magnetic Fields in Magic-Angle Twisted Trilayer Graphene, Phys. Rev. Lett. **127**, 097001 (2021).

[30] Yanhao Tang, Lizhong Li, Tingxin Li, Yang Xu, Song Liu, Katayun Barmak, Kenji Watanabe, Takashi Taniguchi, Allan H. MacDonald, Jie Shan *et al.*, Simulation of Hubbard model physics in WSe2/WS2 moiré superlattices, Nature (London) **579**, 353 (2020).

[31] Juan F. Sierra, Jaroslav Fabian, Roland K. Kawakami, Stephan Roche, and Sergio O. Valenzuela, Van der Waals heterostructures for spintronics and opto-spintronics, Nat. Nanotechnol. **16**, 856 (2021).

[32] Rai Moriya, Naoto Yabuki, and Tomoki Machida, Super-conducting proximity effect in a NbSe_2/graphene van der Waals junction, Phys. Rev. B **101**, 054503 (2020).

[33] Hui Han, Jie Ling, Wenhui Liu, Hui Li, Changjin Zhang, and Jiannong Wang, Superconducting proximity effect in a van der Waals 2H-TaS$_2$/NbSe$_2$ heterostructure, Appl. Phys. Lett. **118**, 253101 (2021).

[34] Klaus Zollner, Martin Gmitra, Tobias Frank, and Jaroslav Fabian, Theory of proximity-induced exchange coupling in graphene on hbn/(Co, Ni), Phys. Rev. B **94**, 155441 (2016).

[35] Klaus Zollner, Martin Gmitra, and Jaroslav Fabian, Electri-cally tunable exchange splitting in bilayer graphene on monolayer Cr$_2$X$_2$Te$_6$ with X = Ge, Si, and Sn, New J. Phys. **20**, 073007 (2018).

[36] Klaus Zollner, Paulo E. Faria Junior, and Jaroslav Fabian, Proximity exchange effects in $MoSe_2$ and WSe_2 hetero-structures with CrI_3: Twist angle, layer, and gate depend-ence, Phys. Rev. B **100**, 085128 (2019).

[37] Klaus Zollner, Paulo E. Faria Junior, and Jaroslav Fabian, Giant proximity exchange and valley splitting in transition metal dichalcogenide/hBN/(Co, Ni) heterostructures, Phys. Rev. B **101**, 085112 (2020).

[38] Ali Hallal, Fatima Ibrahim, Hongxin Yang, Stephan Roche, and Mairbek Chshiev, Tailoring magnetic insulator proximity effects in graphene: First-principles calculations, 2D Mater. **4**, 025074 (2017).

[39] Jiayong Zhang, Bao Zhao, Yugui Yao, and Zhongqin Yang, Robust quantum anomalous Hall effect in gra-phene-based van der Waals heterostructures, Phys. Rev. B **92**, 165418 (2015).

[40] Jiayong Zhang, Bao Zhao, Tong Zhou, Yang Xue, Chunlan Ma, and Zhongqin Yang, Strong magnetization and Chern insulators in compressed graphene/CrI$_3$ van der Waals heterostructures, Phys. Rev. B **97**, 085401 (2018).

[41] H. X. Yang, A. Hallal, D. Terrade, X. Waintal, S. Roche, and M. Chshiev, Proximity Effects Induced in Graphene by Magnetic Insulators: First-Principles Calculations on Spin Filtering and Exchange-Splitting Gaps, Phys. Rev. Lett. **110**, 046603 (2013).

[42] A Dyrdał and J Barnaś, Anomalous, spin, and valley Hall effects in graphene deposited on ferromagnetic substrates, 2D Mater. **4**, 034003 (2017).

[43] Yu Song, Electric-field-induced extremely large change in resistance in graphene ferromagnets, J. Phys. D **51**, 025002 (2018).

[44] Håvard Haugen, Daniel Huertas-Hernando, and Arne Brataas, Spin transport in proximity-induced ferromag-netic graphene, Phys. Rev. B **77**, 115406 (2008).

[45] Jiayong Zhang, Bao Zhao, Yugui Yao, and Zhongqin Yang, Quantum anomalous Hall effect in graphene-based heterostructure, Sci. Rep. **5**, 10629 (2015).

[46] Shanshan Su, Yafis Barlas, Junxue Li, Jing Shi, and Roger K. Lake, Effect of intervalley interaction on band topology of commensurate graphene/EuO heterostructures, Phys. Rev. B **95**, 075418 (2017).

[47] M. Gibertini, M. Koperski, A. F. Morpurgo, and K. S. Novoselov, Magnetic 2D materials and heterostructures, Nat. Nanotechnol. **14**, 408 (2019).

[48] D. R. Klein, D. MacNeill, J. L. Lado, D. Soriano, E. Navarro-Moratalla, K. Watanabe, T. Taniguchi, S. Manni, P. Canfield, J. Fernández-Rossier, and P. Jarillo-Herrero, Probing magnetism in 2D van der Waals crystalline insulators via electron tunneling, Science **360,** 1218 (2018).

[49] C. Cardoso, D. Soriano, N. A. García-Martínez, and J. Fernández-Rossier, Van der Waals Spin Valves, Phys. Rev. Lett. **121,** 067701 (2018).

[50] J. C. G. Henriques, G. Catarina, A. T. Costa, J. Fernández-Rossier, and N. M. R. Peres, Excitonic magneto-optical Kerr effect in two-dimensional transition metal dichalcogenides induced by spin proximity, Phys. Rev. B **101,** 045408 (2020).

[51] Simranjeet Singh, Jyoti Katoch, Tiancong Zhu, Keng Yuan Meng, Tianyu Liu, Jack T. Brangham, Fengyuan Yang, Michael E. Flatté, and Roland K. Kawakami, Strong Modulation of Spin Currents in Bilayer Graphene by Static and Fluctuating Proximity Exchange Fields, Phys. Rev. Lett. **118,** 187201 (2017).

[52] Adrian G. Swartz, Patrick M. Odenthal, Yufeng Hao, Rodney S. Ruoff, and Roland K. Kawakami, Integration of the ferromagnetic insulator EuO onto graphene, ACS Nano **6,** 10063 (2012).

[53] Martin Gmitra and Jaroslav Fabian, Graphene on transition-metal dichalcogenides: A platform for proximity spin-orbit physics and optospintronics, Phys. Rev. B **92,** 155403 (2015).

[54] Martin Gmitra, Denis Kochan, Petra Högl, and Jaroslav Fabian, Trivial and inverted Dirac bands and the emergence of quantum spin Hall states in graphene on transition-metal dichalcogenides, Phys. Rev. B **93,** 155104 (2016).

[55] Klaus Zollner and Jaroslav Fabian, Single and bilayer graphene on the topological insulator Bi_2Se_3: Electronic and spin-orbit properties from first principles, Phys. Rev. B **100,** 165141 (2019).

[56] Klaus Zollner and Jaroslav Fabian, Heterostructures of graphene and topological insulators Bi_2Se_3, Bi_2Te_3, and Sb_2Te_3, Phys. Status Solidi (b) **258,** 2000081 (2021).

[57] Dmitrii Khokhriakov, Anamul Md. Hoque, Bogdan Karpiak, and Saroj P. Dash, Gate-tunable spin-galvanic effect in graphene-topological insulator van der Waals heterostructures at room temperature, Nat. Commun. **11,** 3657 (2020).

[58] Bogdan Karpiak, Aron W. Cummings, Klaus Zollner, Marc Vila, Dmitrii Khokhriakov, Anamul Md Hoque, André Dankert, Peter Svedlindh, Jaroslav Fabian, Stephan Roche, and Saroj P. Dash, Magnetic proximity in a van der Waals heterostructure of magnetic insulator and graphene, 2D Mater. **7,** 015026 (2020).

[59] Simon Zihlmann, Aron W. Cummings, Jose H. Garcia, Máté Kedves, Kenji Watanabe, Takashi Taniguchi, Christian Schönenberger, and Péter Makk, Large spin relaxation anisotropy and valley-Zeeman spin-orbit coupling in WSe_2/graphene/h-BN heterostructures, Phys. Rev. B **97,** 075434 (2018).

[60] Kenan Song, David Soriano, Aron W. Cummings, Roberto Robles, Pablo Ordejón, and Stephan Roche, Spin proximity effects in graphene/topological insulator heterostructures, Nano Lett. **18,** 2033 (2018).

[61] Dmitrii Khokhriakov, Aron W. Cummings, Kenan Song, Marc Vila, Bogdan Karpiak, André Dankert, Stephan Roche, and Saroj P. Dash, Tailoring emergent spin phenomena in Dirac material heterostructures, Sci. Adv. **4,** eaat9349 (2018).

[62] Jose H. Garcia, Marc Vila, Aron W. Cummings, and Stephan Roche, Spin transport in graphene/transition metal dichalcogenide heterostructures, Chem. Soc. Rev. **47,** 3359 (2018).

[63] C. K. Safeer, Josep Ingla-Aynés, Franz Herling, José H. Garcia, Marc Vila, Nerea Ontoso, M. Reyes Calvo, Stephan Roche, Luis E. Hueso, and Fèlix Casanova, Room-temperature spin Hall effect in graphene/MoS_2 van der Waals heterostructures, Nano Lett. **19,** 1074 (2019).

[64] Franz Herling, C. K. Safeer, Josep Ingla-Ayns, Nerea Ontoso, Luis E. Hueso, and Flix Casanova, Gate tunability of highly efficient spin-to-charge conversion by spin Hall effect in graphene proximitized with WSe2, APL Mater. **8,** 071103 (2020).

[65] Jun Yong Khoo, Alberto F. Morpurgo, and Leonid Levitov, On-demand spin-orbit interaction from which-layer tunability in bilayer graphene, Nano Lett. **17,** 7003 (2017).

[66] Zhe Wang, Dong-Keun Ki, Hua Chen, Helmuth Berger, Allan H. MacDonald, and Alberto F. Morpurgo, Strong interface-induced spin-orbit interaction in graphene on WS2, Nat. Commun. **6,** 8339 (2015).

[67] S. Omar and B. J. van Wees, Spin transport in high-mobility graphene on WS_2 substrate with electric-field tunable proximity spin-orbit interaction, Phys. Rev. B **97,** 045414 (2018).

[68] S. Omar and B. J. van Wees, Graphene-WS_2 heterostructures for tunable spin injection and spin transport, Phys. Rev. B **95,** 081404(R) (2017).

[69] Bálint Fülöp, Albin Márffy, Simon Zihlmann, Martin Gmitra, Endre Tóvári, Bálint Szentpéteri, Máté Kedves, Kenji Watanabe, Takashi Taniguchi, Jaroslav Fabian *et al.,* Boosting proximity spin-orbit coupling in graphene/WSe2 heterostructures via hydrostatic pressure, npj 2D Mater. Appl. **5,** 82 (2021).

[70] Klaus Zollner, Marko D. Petrović, Kapildeb Dolui, Petr Plecháč, Branislav K. Nikolić, and Jaroslav Fabian, Scattering-induced and highly tunable by gate damping-like spin-orbit torque in graphene doubly proximitized by two-dimensional magnet $Cr_2Ge_2Te_6$ and monolayer WS_2, Phys. Rev. Research **2,** 043057 (2020).

[71] M Umar Farooq and Jisang Hong, Switchable valley splitting by external electric field effect in graphene/CrI_3 heterostructures, npj 2D Mater. Appl. **3,** 3 (2019).

[72] Kyle L. Seyler, Ding Zhong, Bevin Huang, Xiayu Linpeng, Nathan P. Wilson, Takashi Taniguchi, Kenji Watanabe, Wang Yao, Di Xiao, Michael A. McGuire, Kai-Mei C. Fu, and Xiaodong Xu, Valley manipulation by optically tuning the magnetic proximity effect in WSe2/CrI3 heterostructures, Nano Lett. **18,** 3823 (2018).

[73] Zhiyong Wang, Chi Tang, Raymond Sachs, Yafis Barlas, and Jing Shi, Proximity-Induced Ferromagnetism in

Graphene Revealed by the Anomalous Hall Effect, Phys. Rev. Lett. **114**, 016603 (2015).

[74] J. B. S. Mendes, O. Alves Santos, L. M. Meireles, R. G. Lacerda, L. H. Vilela-Leão, F. L. A. Machado, R. L. Rodríguez-Suárez, A. Azevedo, and S. M. Rezende, Spin-Current to Charge-Current Conversion and Magneto-resistance in a Hybrid Structure of Graphene and Yttrium Iron Garnet, Phys. Rev. Lett. **115**, 226601 (2015).

[75] Johannes Christian Leutenantsmeyer, Alexey A. Kaverzin, Magdalena Wojtaszek, and Bart J. van Wees, Proximity induced room temperature ferromagnetism in graphene probed with spin currents, 2D Mater. **4**, 014001 (2016).

[76] Klaus Zollner, Martin Gmitra, and Jaroslav Fabian, Swapping Exchange and Spin-Orbit Coupling in 2D van der Waals Heterostructures, Phys. Rev. Lett. **125**, 196402 (2020).

[77] The acronym "ex-so-tic" accounts for heterostructures with both proximity-induced spin interactions, exchange (ex) and spinorbit (so) coupling.

[78] Kapildeb Dolui, Marko D. Petrovic, Klaus Zollner, Petr Plechac, Jaroslav Fabian, and Branislav K. Nikolic, Proximity spin–orbit torque on a two-dimensional magnet within van der Waals heterostructure: Current-driven anti-ferromagnet-to-ferromagnet reversible nonequilibrium phase transition in bilayer CrI_3, Nano Lett. **20**, 2288 (2020).

[79] Mohammed Alghamdi, Mark Lohmann, Junxue Li, Palani R. Jothi, Qiming Shao, Mohammed Aldosary, Tang Su, Boniface P. T. Fokwa, and Jing Shi, Highly efficient spin-orbit torque and switching of layered ferromagnet Fe_3GeTe_2, Nano Lett. **19**, 4400 (2019).

[80] Xiao Wang *et al.*, Current-driven magnetization switching in a van der Waals ferromagnet Fe_3GeTe_2, Sci. Adv. **5**, eaaw8904 (2019).

[81] Predrag Lazić, K. D. Belashchenko, and Igor Žutić, Effective gating and tunable magnetic proximity effects in two-dimensional heterostructures, Phys. Rev. B **93**, 241401(R) (2016).

[82] Shiming Yan, Shengmei Qi, Dunhui Wang, and Wenbo Mi, Novel electronic structures and magnetic properties in twisted two-dimensional graphene/Janus 2H-VHeTe heterostructures, Physica (Amsterdam) **134E**, 114854 (2021).

[83] Alessandro David, Péter Rakyta, Andor Kormányos, and Guido Burkard, Induced spin-orbit coupling in twisted graphene–transition metal dichalcogenide heterobilayers: Twistronics meets spintronics, Phys. Rev. B **100**, 085412 (2019).

[84] Yang Li and Mikito Koshino, Twist-angle dependence of the proximity spin-orbit coupling in graphene on transition-metal dichalcogenides, Phys. Rev. B **99**, 075438 (2019).

[85] See Supplemental Material at http://link.aps.org/supplemental/10.1103/PhysRevLett.128.106401 where we show a more extended summary of results, which includes Refs. [4,34,39,58,69,70,75,82,83,87,90,92–113].

[86] Bálint Fülöp, Albin Márffy, Endre Tóvári, Máté Kedves, Simon Zihlmann, David Indolese, Zoltán Kovács-Krausz, Kenji Watanabe, Takashi Taniguchi, Christian Schönenberger *et al.*, New method of transport measurements on van der Waals heterostructures under pressure, J. Appl. Phys. **130**, 064303 (2021).

[87] Petra Högl, Tobias Frank, Klaus Zollner, Denis Kochan, Martin Gmitra, and Jaroslav Fabian, Quantum Anomalous Hall Effects in Graphene from Proximity-Induced Uniform and Staggered Spin-Orbit and Exchange Coupling, Phys. Rev. Lett. **124**, 136403 (2020).

[88] S. R. Bahn and K. W. Jacobsen, An object-oriented scripting interface to a legacy electronic structure code, Comput. Sci. Eng. **4**, 56 (2002).

[89] Predrag Lazic, Cellmatch: Combining two unit cells into a common supercell with minimal strain, Comput. Phys. Commun. **197**, 324 (2015).

[90] Daniel S. Koda, Friedhelm Bechstedt, Marcelo Marques, and Lara K. Teles, Coincidence lattices of 2d crystals: heterostructure predictions and applications, J. Phys. Chem. C **120**, 10895 (2016).

[91] Y. Baskin and L. Meyer, Lattice constants of graphite at low temperatures, Phys. Rev. **100**, 544 (1955).

[92] V. Carteaux, D. Brunet, G. Ouvrard, and G. Andre, Crystallographic, magnetic and electronic structures of a new layered ferromagnetic compound $Cr_2Ge_2Te_6$, J. Phys. Condens. Matter **7**, 69 (1995).

[93] P. Hohenberg and W. Kohn, Inhomogeneous electron gas, Phys. Rev. **136**, B864 (1964).

[94] Paolo Giannozzi *et al.*, Quantum espresso: A modular and open-source software project for quantum simulations of materials, J. Phys. Condens. Matter **21**, 395502 (2009).

[95] Cheng Gong, Lin Li, Zhenglu Li, Huiwen Ji, Alex Stern, Yang Xia, Ting Cao, Wei Bao, Chenzhe Wang, Yuan Wang, Z. Q. Qiu, R. J. Cava, Steven G. Louie, Jing Xia, and Xiang Zhang, Discovery of intrinsic ferromagnetism in two-dimensional van der Waals crystals, Nature (London) **546**, 265 (2017).

[96] G. Kresse and D. Joubert, From ultrasoft pseudopotentials to the projector augmented-wave method, Phys. Rev. B **59**, 1758 (1999).

[97] John P. Perdew, Kieron Burke, and Matthias Ernzerhof, Generalized Gradient Approximation Made Simple, Phys. Rev. Lett. **77**, 3865 (1996).

[98] Stefan Grimme, Semiempirical GGA-type density functional constructed with a long-range dispersion correction, J. Comput. Chem. **27**, 1787 (2006).

[99] Stefan Grimme, Jens Antony, Stephan Ehrlich, and Helge Krieg, A consistent and accurate ab initio parametrization of density functional dispersion correction (DFT-D) for the 94 elements H-Pu, J. Chem. Phys. **132**, 154104 (2010).

[100] Vincenzo Barone, Maurizio Casarin, Daniel Forrer, Michele Pavone, Mauro Sambi, and Andrea Vittadini, Role and effective treatment of dispersive forces in materials: Polyethylene and graphite crystals as test cases, J. Comput. Chem. **30**, 934 (2009).

[101] Lennart Bengtsson, Dipole correction for surface supercell calculations, Phys. Rev. B **59**, 12301 (1999).

[102] Xingxing Li and Jinlong Yang, $CrXTe_3$ ($X = Si$, Ge) nanosheets: Two dimensional intrinsic ferromagnetic semiconductors, J. Mater. Chem. C **2**, 7071 (2014).

[103] Xiaofang Chen, Jingshan Qi, and Daning Shi, Strain-engineering of magnetic coupling in two-dimensional magnetic semiconductor CrSiTe3: Competition of direct exchange interaction and superexchange interaction, Phys. Lett. A **379**, 60 (2015).

[104] Lifei Liu, Xiaohui Hu, Yifeng Wang, Arkady V. Krasheninnikov, Zhongfang Chen, and Litao Sun, Tunable electronic properties and enhanced ferromagnetism in Cr2Ge2Te6 monolayer by strain engineering, Nanotechnology **32**, 485408 (2021).

[105] Talieh S. Ghiasi, Alexey A. Kaverzin, Avalon H. Dismukes, Dennis K. de Wal, Xavier Roy, and Bart J. van Wees, Electrical and thermal generation of spin currents by magnetic bilayer graphene, Nat. Nanotechnol. **16**, 788 (2021).

[106] Matthew R. Rosenberger, Hsun-Jen Chuang, Madeleine Phillips, Vladimir P. Oleshko, Kathleen M. McCreary, Saujan V. Sivaram, C. Stephen Hellberg, and Berend T. Jonker, Twist angle-dependent atomic reconstruction and moiré patterns in transition metal dichalcogenide heterostructures, ACS Nano **14**, 4550 (2020).

[107] Astrid Weston, Yichao Zou, Vladimir Enaldiev, Alex Summerfield, Nicholas Clark, Viktor Zólyomi, Abigail Graham, Celal Yelgel, Samuel Magorrian, Mingwei Zhou *et al.*, Atomic reconstruction in twisted bilayers of transition metal dichalcogenides, Nat. Nanotechnol. **15**, 592 (2020).

[108] Tribhuwan Pandey, Avinash P. Nayak, Jin Liu, Samuel T. Moran, Joon-Seok Kim, Lain-Jong Li, Jung-Fu Lin, Deji Akinwande, and Abhishek K. Singh, Pressure-induced charge transfer doping of monolayer graphene/MoS_2 heterostructure, Small **12**, 4063 (2016).

[109] Klaus Zollner and Jaroslav Fabian, Bilayer graphene encapsulated within monolayers of WS_2 or $Cr_2Ge_2Te_6$: Tunable proximity spin-orbit or exchange coupling, Phys. Rev. B **104**, 075126 (2021).

[110] Denis Kochan, Susanne Irmer, and Jaroslav Fabian, Model spin-orbit coupling Hamiltonians for graphene systems, Phys. Rev. B **95**, 165415 (2017).

[111] Võ Tien Phong, Niels R. Walet, and Francisco Guinea, Effective interactions in a graphene layer induced by the proximity to a ferromagnet, 2D Mater. **5**, 014004 (2017).

[112] Thomas Naimer, Klaus Zollner, Martin Gmitra, and Jaroslav Fabian, Twist-angle dependent proximity induced spin-orbit coupling in graphene/transition metal dichalcogenide heterostructures, Phys. Rev. B **104**, 195156 (2021).

[113] Armando Pezo, Zeila Zanolli, Nils Wittemeier, Pablo Ordejón, Adalberto Fazzio, Stephan Roche, and Jose H. Garcia, Manipulation of spin transport in graphene/transition metal dichalcogenide heterobilayers upon twisting, 2D Mater. **9**, 015008 (2022).

[114] Marc Vila, Jose H. Garcia, and Stephan Roche, Valley-polarized quantum anomalous Hall phase in bilayer graphene with layer-dependent proximity effects, Phys. Rev. B **104**, L161113 (2021).